RAA 2015 Vol. **15** No. **1**, 117–126 doi: 10.1088/1674–4527/15/1/011
http://www.raa-journal.org *http://www.iop.org/journals/raa*

***R**esearch in*
***A**stronomy and*
***A**strophysics*

Long-term transit timing monitoring and homogenous study of WASP-32 *

Lei-Lei Sun[1,2,4], Sheng-Hong Gu[1,2], Xiao-Bin Wang[1,2], Andrew Collier Cameron[3], Dong-Tao Cao[1], Yi-Bo Wang[1], Yue Xiang[1,4], Ho-Keung Hui[5], Chi-Tai Kwok[5], Bill Yeung[6] and Kam-Cheung Leung[6]

[1] Yunnan Observatories, Chinese Academy of Sciences, Kunming 650011, China; *wangxb@ynao.ac.cn*
[2] Key Laboratory for the Structure and Evolution of Celestial Objects, Chinese Academy of Sciences, Kunming 650011, China
[3] School of Physics and Astronomy, University of St Andrews, North Haugh, St Andrews, Fife KY16 9SS, UK
[4] University of Chinese Academy of Sciences, Beijing 100049, China
[5] Ho Koon Nature Education cum Astronomical Centre, Sik Sik Yuen, Hong Kong, China
[6] Hong Kong Astronomical Society, Hong Kong, China

Received 2014 January 22; accepted 2014 May 28

Abstract We report new photometric observations of the transiting exoplanetary system WASP-32 made by using CCD cameras at Yunnan Observatories and Ho Koon Nature Education cum Astronomical Centre, China from 2010 to 2012. Following our usual procedure, the observed data are corrected for systematic errors according to the coarse decorrelation and SYSREM algorithms so as to enhance the signal of the transit events. Combined with radial velocity data presented in the literature, our newly observed data and earlier photometric data in the literature are simultaneously analyzed to derive the physical parameters describing the system by employing the Markov chain Monte Carlo technique. The derived parameters are consistent with the result published in the original paper about WASP-32b, but the uncertainties of the new parameters are smaller than those in the original paper. Moreover, our modeling result supports a circular orbit for WASP-32b. Through the analysis of all available mid-transit times, we have refined the orbital period of WASP-32b; no evident transit timing variation is found in these transit events.

Key words: techniques: photometric — transiting exoplanetary system — individual: WASP-32

1 INTRODUCTION

The photometric transit survey has been shown to be one of the most successful methods for discovering extrasolar planetary systems over the past decade, yielding 615 planetary systems which

* Supported by the National Natural Science Foundation of China.

have been found to contain 350 multiple planetary systems up to 2014 May 28.[1] Moreover, photometric observation of a transiting system is the only way to directly measure the size and mass of the exoplanet, combined with radial velocity observation. The follow-up observations for the known transiting exoplanetary system can not only improve the parameters describing the system, but also provide us with important information about the existence of additional bodies in the system with the transit timing variation (TTV) method (Miralda-Escudé 2002; Agol et al. 2005; Holman & Murray 2005) and/or transit duration variation (TDV) method (Kipping 2009). Through the analysis of long-term monitoring of TTV and/or TDV for transiting exoplanetary systems, even based on current ground-based measurements, terrestrial planets have become easily detectable, even though they are difficult to detect with other methods (Agol et al. 2005; Holman & Murray 2005). All of the above information is significant for the study of planetary properties, such as the composition, structure and scenario of planetary system formation and evolution (Baraffe et al. 2008, 2010; Enoch et al. 2012). Therefore, since 2007, we have run a monitoring project for some known transiting exoplanetary systems by using the 1 m and 2.4 m telescopes at Yunnan Observatories (YO, hereafter) and the 0.5 m telescope at Ho Koon Nature Education cum Astronomical Centre (HKNEAC, hereafter) in China, and already published a series of observational results about HAT-P-24, HAT-P-8 and WASP-11/HAT-P-10 (Wang et al. 2013; Tan et al. 2013; Wang et al. 2014).

WASP-32b was discovered by Maxted et al. (2010); it is a massive hot Jupiter with a mass of $3.60 \pm 0.07\,M_{\rm Jup}$ and a radius of $1.18 \pm 0.07\,R_{\rm Jup}$. Its host star is a Sun-like, lithium-depleted, main-sequence star. Later, Sada et al. (2012) obtained a complete J-band light curve of WASP-32 by utilizing the 2.1 m telescope at Kitt Peak National Observatory (KPNO, hereafter) on 2011 October 15. Then, relying on the newly obtained photometric and spectroscopic data, Brown et al. (2012) recalculated the parameters of the system and measured the spin-orbit alignment angle by analyzing the Rossiter-McLaughlin (R-M) effect for WASP-32. In 2014, Brothwell et al. confirmed the result of Brown et al. (2012) on the R-M effect (Brothwell et al. 2014). We have monitored this system at YO since 2010; one partial transit light curve and two complete ones have been recorded. In addition, we acquired a partial transit light curve at HKNEAC in 2011. Here, we present our analysis result of transiting system WASP-32 based on our new photometric observations, available light curves and the radial velocity curves in the literature (Maxted et al. 2010; Brown et al. 2012; Sada et al. 2012).

In Section 2, we describe our observations and data reduction approach. In Section 3, we introduce the stellar atmospheric parameters of WASP-32, which are used to solve the physical parameters of the system. In Section 4, an analysis of the system is performed by employing the Markov chain Monte Carlo (MCMC) technique, and the orbital period is improved through observed minus calculated $(O - C)$ analysis. In Section 5, we discuss the new results. Finally, we summarize our new study in Section 6.

2 OBSERVATIONS AND DATA REDUCTION

2.1 Photometric Observations with YO-1 m Telescope

WASP-32 was observed using the Andor 2k×2k CCD camera attached to the 1 m telescope at YO, China, on 2010 November 6, 2011 October 31 and 2012 November 20. During the three observation runs, the standard R filter was used and the field of view was $7.3 \times 7.3\ \mathrm{arcmin}^2$. Additionally, the exposure times were appropriately set according to weather conditions (see Table 1). In the first observation run, the weather was photometric and the seeing was good; the status of the instrument was also fine. In the second observation run, some thin clouds intermittently appeared in the sky but the observation could still be carried out until the tracking system of the telescope was interrupted because of a technical problem. In the third observation run, the weather was clear and the seeing was good; the status of the instrument was also fine. During the above three observation runs, because

[1] *http://exoplanet.eu/catalog/*

Table 1 The Observation Log of WASP-32

Date (UT)	Equipment	Filter	Airmass	Exposure Time (s)	rms (mag)
2010.11.06	YO-1 m	R	1.12–2.04	40–60	0.0028
2011.10.31	YO-1 m	R	1.76–1.12	120–180	0.0019
2011.12.19	HKNEAC-0.5 m	R	1.08–1.02	60–90	0.0023
2012.11.20	YO-1 m	R	1.25–1.09–2.09	60–90	0.0020

Notes: rms means the root mean square of the residuals between the reduced observational data and the fitting model of the light curve.

there was no auto-guiding system in the telescope, the centroids of star images drifted by a few pixels on the CCD image from time to time. In order to minimize the systematic error induced by this issue, we manually adjusted the position of the target star to the initial one every several images.

2.2 Photometric Observation with HKNEAC-0.5 m Telescope

On 2011 December 19, WASP-32 was observed by utilizing the Apogee 3k×3k CCD camera attached to the 0.5 m telescope at HKNEAC, China. During the observation, the standard R filter was used and the field of view was $31.4 \times 31.4\ \mathrm{arcmin}^2$. The weather was good for photometric observation at first, but the observation was forced to terminate later when thick clouds appeared in the sky.

2.3 Data Reduction

We perform the data reduction by utilizing the same procedure as was described in detail by Wang et al. (2013). Namely, the observed CCD images of both instruments are reduced by means of the IRAF package, including image trimming, bias subtraction, dark current subtraction (which is only implemented for observational images taken by the HKNEAC-0.5 m telescope), flat-field correction and cosmic ray removal. For the different sizes of the field of view of the YO-1 m and HKNEAC-0.5 m telescopes, we appropriately select 8 and 42 reference stars from the two instruments respectively. After the above reduction, values of instrumental magnitude for the target star and reference stars are measured by utilizing the APPHOT sub-package of IRAF. In the measurements, we tried a series of apertures to conduct the aperture photometry and eventually chose the optimal apertures for minimizing the dispersion of light curves.

2.4 Systematic Error Correction

Because the amplitude of light variation of a host star induced by the transiting exoplanet is normally small, we use coarse decorrelation and SYSREM methods to correct the systematic errors in the photometric data in order to reinforce the signal of transit events (Collier Cameron et al. 2006; Tamuz et al. 2005; Wang et al. 2013). First, the photometric data of all reference stars are iteratively analyzed with the coarse decorrelation method, during which the error of each reference star is properly estimated considering the photometric errors from IRAF, based on a maximum-likelihood approach (Collier Cameron et al. 2006). Second, these high-quality reference stars are used to model the systematic errors in the photometric data with the SYSREM method, which are successively corrected in the data of the target star. Third, there are some systematic trends still left in the target star's data because of the different extinctions between target and reference stars, so we use a linear function or a quadratic one to fit the out-of-transit data for the trend and individually remove them from the light curve. Finally, we convert the local observation time into the Barycentric Julian Date based on the Coordinated Universal Time ($\mathrm{BJD_{UTC}}$). After finishing the above procedure, we derive the final light curves of the transit events of WASP-32, which are used to analyze the physical parameters of the system in Section 4.

3 THE STELLAR PARAMETERS OF WASP-32

Stellar parameters play a key role in characterizing the properties of a planetary system. In order to derive the masses and radii of a host star and its planet, we need some other constraints besides the transit light curves and radial velocity curves of the host star, which can usually be derived in two ways: (1) interpolate the stellar evolutionary model grids with the stellar atmospheric parameters, namely effective temperature $T_{\rm eff}$, metallicity [Fe/H] and stellar mean density (or scaled semimajor axis of the orbit with stellar radius a/R_*), to acquire the stellar mass and radius (Torres et al. 2008; Seager & Mallén-Ornelas 2003; Sozzetti et al. 2007; Yi et al. 2001); (2) with the above two stellar atmospheric parameters and additional stellar surface gravity log g_*, take advantage of the calibration of Torres et al. (2010), which was subsequently improved by Enoch et al. (2010), who substituted log g_* with the stellar mean density, to obtain the stellar mass and radius. The second method has been used in our analysis for physical parameters of the host star by employing the MCMC technique (Enoch et al. 2010).

For WASP-32, two sets of stellar atmospheric parameters (see Table 2) were independently derived based on the observations from two spectrographs using different spectral analysis methods (Maxted et al. 2010; Mortier et al. 2013), which are different from each other. Thus, we need to estimate the qualities of these two results by comparing the stellar mean density derived from spectroscopic atmospheric parameters based on the calibration of Torres et al. (2010) with this one, derived by modeling the photometric light curves. To model the shape of the light curves, the limb-darkening coefficients are very important; these depend on the stellar atmospheric parameters. We investigate the influences of two sets of atmospheric parameters on the light curve model with the small planet approximation of Mandel & Agol (2002) and find that the differences in the simulated light curves based on these two sets of atmospheric parameters among all three observational filters (e.g. R, J, z) are smaller than 3×10^{-5} magnitude, and are indistinguishable compared with the observational precisions. Therefore, we confirm that the mean densities of the host star from Maxted et al. (2010) and Brown et al. (2012) could be treated as reference values for comparison. We derive the stellar mean densities based on these two sets of atmospheric parameters using the calibration of Torres et al. (2010) and compare them with the values of Maxted et al. (2010) and Brown et al. (2012). The result demonstrates that the derived stellar density from the atmospheric parameters of Maxted et al. (2010) is in agreement with the above reference values, but that from the atmospheric parameters of Mortier et al. (2013) is larger than the above reference values. As Torres et al. (2012) mentioned, the surface gravity is difficult to measure accurately because of its rather subtle effect on the spectral profile. Therefore, we can give a reasonable interpretation for all three larger values of Mortier et al. (2013), because they overestimated the surface gravity of the host star. In the following analysis, we select the stellar atmospheric parameters of Maxted et al. (2010) as the final input parameters.

Table 2 Stellar Atmospheric Parameters of WASP-32

Parameter (unit)	Maxted et al. (2010)	Mortier et al. (2013)
Effective temperature $T_{\rm eff}$ (K)	6100 ± 100	6427 ± 141
Surface gravity log g_*	4.4 ± 0.2	4.93 ± 0.08
Metallicity [Fe/H]	-0.13 ± 0.1	0.28 ± 0.10
Microturbulence $\xi_t (\rm km\ s^{-1})$	1.2 ± 0.1	1.20 ± 0.21

4 LIGHT CURVE ANALYSIS

First, we briefly introduce the employed MCMC technique (see Collier Cameron et al. (2007) and Pollacco et al. (2008) for more details), which simultaneously estimates the photometric model of an exoplanet transit event and the radial velocity model of the reflex motion of the host star induced by the companion planet.

The present version of this MCMC code can be used for both cases of eccentric and circular orbits. There are eight free parameters in this calculation, namely the orbital period P, the mid-transit time T_c, the transit duration T_{14}, the planet/star area ratio ΔF, the impact parameter b, the semi-amplitude of radial velocity curve K_1, the orbital eccentricity e and the argument of periastron ω. However, the last two parameters are not directly used in the code, but substituted by $e\cos\omega$ and $e\sin\omega$, which could accelerate the convergence of MCMC computation (Ford 2005; Anderson et al. 2011). Moreover, the calibration of Enoch et al. (2010) is utilized in the code to infer the mass of the host star as described above. The light curves are modeled based on the small planet approximation and a four-coefficient limb-darkening law is used (Mandel & Agol 2002). The four limb-darkening coefficients are derived through interpolation of the coefficient tables of Claret (2000, 2004). The best fitting values and uncertainties are inferred from the posterior probability distributions of the system parameters.

The mid-transit time T_c is a unique piece of information related to each transit event; its accuracy cannot be improved by combining the data from different transit events. Moreover, the conventional residual permutation method, which is implemented in the MCMC code of Collier Cameron et al. (2007), usually underestimates the actual errors of photometric data (Winn et al. 2008; Carter & Winn 2009). Therefore, in order to reliably analyze the TTV later, we also apply the Transit Analysis Package (TAP) developed by Gazak et al. (2011) to calculate T_c, which utilizes a wavelet-based method to analyze all photometric data sets to account for possible temporally correlated noise (Carter & Winn 2009). Employing these two codes based on the MCMC technique could provide us with more reliable estimations of the uncertainties of the mid-transit times.

4.1 Initial MCMC Analysis

Besides our own four new R-band light curves, we also collect z-band and J-band light curves of Maxted et al. (2010) and Sada et al. (2012) respectively, and two radial velocity curves from the literature (Maxted et al. 2010; Brown et al. 2012). By combining all the light curves with the two radial velocity curves, we can derive the homogenous solution of the system.

First, we calculate the global solution of the system with all available data using the MCMC code of Collier Cameron et al. (2007), during which we run 11 chains with different inputs of some free parameters. We check the posterior probability distributions of several of the main physical parameters and confirm the convergence of the solution through the fact that these chains have similar distributions for these parameters.

Second, the above 11 chains are jointly used to derive the optimal solution. We find that $e\cos\omega$ and $e\sin\omega$ are non-zero at the 1.1σ and 0.3σ levels respectively ($e\cos\omega$=-0.0029 ± 0.0026; $e\sin\omega$=$0.0015^{+0.0057}_{-0.0055}$), whereas the significance levels of Maxted et al. (2010) reach 4σ and 0.7σ, respectively. In addition, we find a 60% probability that our fitted eccentricity could have arisen by chance if the underlying orbit is actually circular by applying the F-test of Lucy & Sweeney (1971). Therefore, we have confidence that the orbit of WASP-32b is circular and a circular orbit is adopted in all the following analyses.

Additionally, we utilize the TAP code to study the system and find that the initial solutions of both codes are in good agreement with those of Maxted et al. (2010) and Sada et al. (2012), respectively.

4.2 The Analysis of Mid-transit Times of WASP-32

In order to examine whether the TTV exists in transiting exoplanet WASP-32b or not, we collect all the available mid-transit times with high precision from the literature and the website, which are determined from the complete/symmetric light curves with higher photometric precision. We find five mid-transit times from the Exoplanet Transit Database (ETD) website[2]. Three new mid-transit times are derived from the above analysis on our two complete R-band light curves and that of Sada et al. (2012) using the code of Collier Cameron et al. (2007) and the TAP. Hereafter, we label the MCMC code of Collier Cameron et al. (2007) as M1 and the TAP code as M2. All available mid-transit times are listed in Table 3.

Table 3 Mid-transit Times of WASP-32b

Cycle	$\mathrm{BJD_{UTC}}$ –2450000	Uncertainty	Theoretical precision	$(O-C)$ (d)	Source
–130	5496.32574	0.00101		0.00085	ETD
–128	5501.76288	0.00129		0.00066	ETD
–126	5507.19973	0.00074	0.00051	0.00018	This work (M1)
–126	5507.19934	0.00187	0.00051	−0.00048	This work (M2)
–17	5803.53419	0.00072		0.00018	ETD
–17	5803.53428	0.00076		0.00027	ETD
0	5849.75051	0.00046	0.00038	−0.00080	Sada et al. (M1)
0	5849.75088	0.00069	0.00038	−0.00060	Sada et al. (M2)
148	6252.11415	0.00063	0.00049	0.00044	This work (M1)
148	6252.11417	0.00139	0.00049	0.00041	This work (M2)
248	6523.98036	0.00093		0.00017	ETD

Considering a series of continuous photometric observations with uncorrelated Gaussian uncertainties of magnitude σ_{ph}, taken at a rate Γ around a single transit, the precision of the mid-transit time is approximately $(t_e/2\Gamma)^{1/2}\sigma_{\mathrm{ph}}\rho^{-2}$ given by Ford & Gaudi (2006), where t_e is the duration of ingress/egress and ρ is the ratio of the planet radius to the stellar radius. We calculate the theoretical precision of our two mid-transit times and that of Sada et al. (2012) using the above formula. Probably because of not considering the correlated noise, the theoretical precision of these mid-transit times is consistently smaller than the uncertainties derived from both M1 and M2, and in particular much smaller than the result from M2 (see Table 3).

We separate the mid-transit times in Table 3 into two data sets according to the relative method and use a linear ephemeris formula $T = T_0 + P * E$ to fit them so as to derive the orbital period values individually, where T_0 indicates the zero point, E means the orbital cycle and P is the orbital period. The relative $(O-C)$ diagrams are shown in Figures 1 and 2. We have found that both of the linear ephemeris formulae could perfectly characterize the mid-transit times with deviations comparable to 1σ in our measurements, especially for the result derived by the M2. Meanwhile, the derived ephemeris formulae are in good agreement with each other. Therefore, there is no apparent transit timing variation based on these available data. Nonetheless, based on our analysis for the mid-transit times, we have derived a more accurate orbital period for WASP-32b.

4.3 Final MCMC Analysis

In this subsection, we adopt the same strategy as in Section 4.1, namely, combining six available light curves with two radial velocity curves to derive the physical parameters of WASP-32, but fixing the orbital period at the above newly derived value and adopting the model that incorporates a circular orbit. It should be noticed that we have adopted the orbital period value from the M1 data

[2] *http://var.astro.cz/ETD*

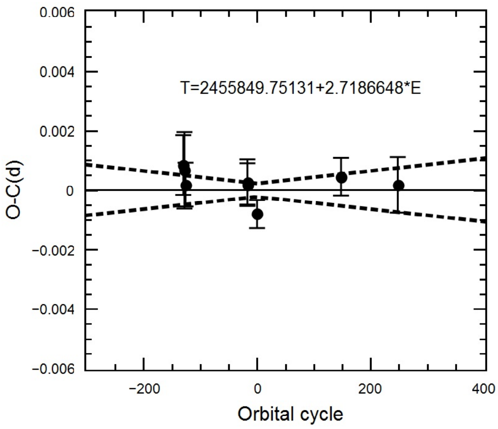

Fig. 1 The $(O-C)$ result based on the mid-transit times calculated by using M1.

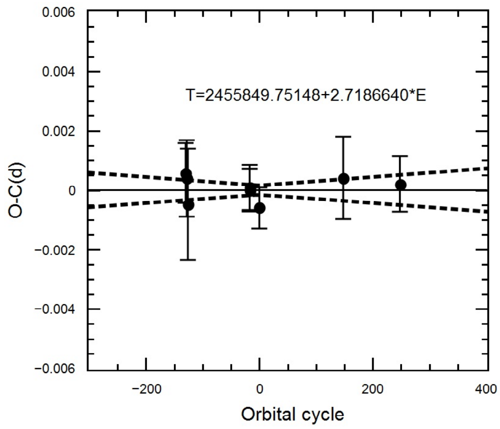

Fig. 2 The $(O-C)$ result based on the mid-transit times calculated by employing M2.

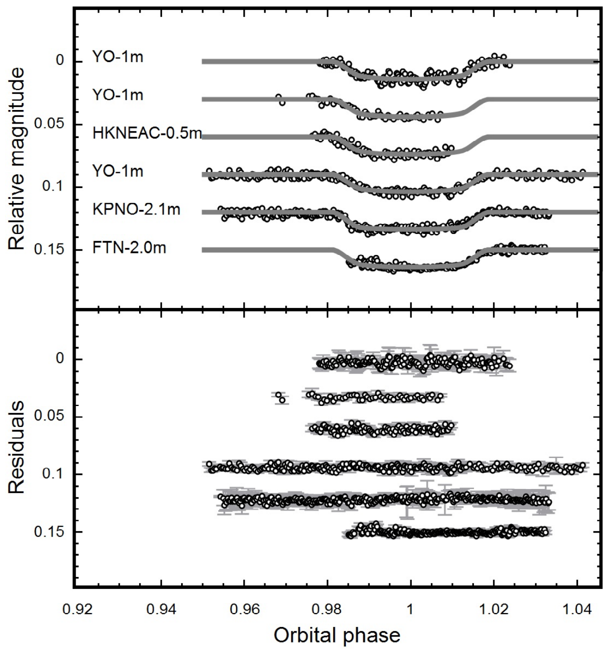

Fig. 3 The final model fitting of light curves and related residuals.

set. Using the MCMC code of Collier Cameron et al. (2007), we generate several chains to ensure the convergence of the solution and derive the optimal solution. The final solution of the physical parameters of WASP-32 is tabulated in Table 4 together with the result of Maxted et al. (2010). The relative model fittings are illustrated in Figures 3 and 4.

Table 4 Physical Parameters of WASP-32

Parameter	This work	Maxted et al. (2010)	Note
T_0(BJD$_{\rm UTC}$ −2450000)	5779.06604 ±0.00020	5151.05460 ±0.00050	Transit epoch
P (d)	2.7186648 ±0.0000016	2.7186590 ±0.0000080	Orbital period
ΔF	0.0121±0.0002	0.0124±0.0004	Planet/star area ratio
T_{14} (d)	0.100 ± 0.001	0.101 ± 0.002	Transit duration
b	$0.671^{+0.023}_{-0.026}$	0.628 ± 0.004	Impact parameter
K_1 (m s^{-1})	483.4 ± 2.6	478 ± 11	Semi-amplitude of radial velocity curve
γ (m s^{-1})	18280.79 ± 0.06	18281 ± 1	Center-of-mass velocity
e	0 (adopted)	0.018 ± 0.0065	Orbital eccentricity
i (°)	85.0 ± 0.3	85.3 ± 0.5	Orbital inclination
a (AU)	0.0395 ± 0.0003	0.0394 ± 0.0003	Orbital separation
$M_*(M_\odot)$	1.112 ± 0.026	1.10 ± 0.03	Stellar mass
$R_*(R_\odot)$	1.113 ± 0.036	1.11 ± 0.05	Stellar radius
$\rho_*(\rho_\odot)$	0.81 ± 0.07	0.80 ± 0.10	Stellar mean density
$M_{\rm p}(M_{\rm Jup})$	3.59 ± 0.06	3.60 ± 0.07	Planet mass
$R_{\rm p}(R_{\rm Jup})$	1.190 ± 0.047	1.18 ± 0.07	Planet radius
$\rho_{\rm p}(\rho_{\rm Jup})$	$2.13^{+0.27}_{-0.22}$	2.2 ± 0.4	Planet mean density
$T_{\rm eq}$ (K)	1571^{+34}_{-36}	1560 ± 50	Planet temperature

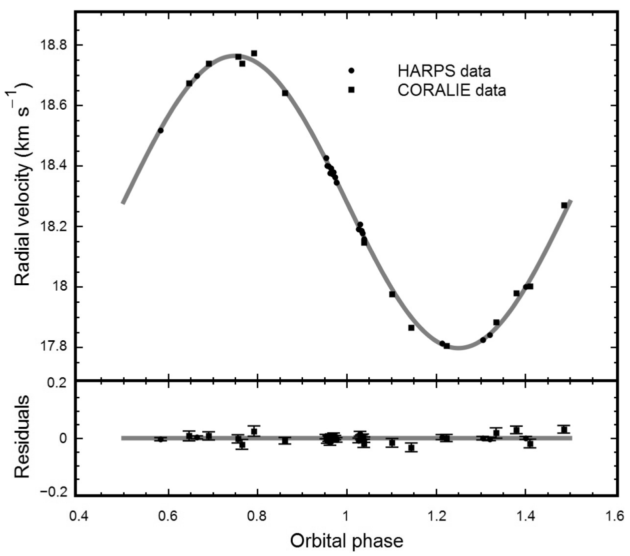

Fig. 4 The final model fitting of radial velocity curves and related residuals.

5 DISCUSSION

Based on the new photometric data and the published photometric and radial velocity data, we have derived the homogenous physical parameters of the transiting exoplanetary system WASP-32. Compared with the result of Maxted et al. (2010) (see Table 4), the new parameters are in good agreement with those of Maxted et al. (2010) except for the impact parameter b. We find that our measurement of b is larger than that of Maxted et al. (2010). Nonetheless, our impact parameter value is consistent with that of Brown et al. (2012), which is derived from the analysis of the R-

M effect, namely the distortion of the radial velocity curve induced by the transiting of the planet, combined with the modeling of light curves, and thus is more reliable. When fitting all mid-transit times of the M1 data set, we obtain a reduced χ^2_ν of 0.785. Then we reevaluate the uncertainties of T_0 and P using the residual permutation method as performed in the code of Collier Cameron et al. (2007), namely using $\sqrt{\chi^2_\nu}\sigma_{T_0}$ and $\sqrt{\chi^2_\nu}\sigma_P$ to estimate the uncertainties in both parameters. In order to examine the goodness of fit, we investigate the accumulation of uncertainties in T_0 and P and show the result in Figure 1, in which we find that all the data points fall in the probable zone of error accumulation (the zone between the dashed lines in Fig. 1) within the 1.2σ level. For the case related to the M2 data set, we derive a reduced χ^2_ν of 0.23 and the adopted uncertainties of T_0 and P ($\sqrt{\chi^2_\nu}\sigma_{T_0} = 1.57585 \times 10^{-4}$; $\sqrt{\chi^2_\nu}\sigma_P = 1.421 \times 10^{-6}$). In Figure 2, all the data points fall in the probable zone of error accumulation within a range smaller than 1σ of the mid-transit times.

As seen from Table 3, the formula of Ford & Gaudi (2006) and the MCMC code of Collier Cameron et al. (2007) supply narrower and more conservative uncertainties of the mid-transit times in comparison with the TAP code. Meanwhile, the estimation of mid-transit times and errors supplied by TAP are considered to be relatively more reliable than other methods that are widely employed. We therefore have confidence that two smallish χ^2_ν, compared to the systems with significant TTV signal (Maciejewski et al. 2010; Jiang et al. 2013; Maciejewski et al. 2013), are not induced by overestimated errors of the mid-transit times and thus probably reveal the absence of TTV in WASP-32 during these transit events. It should be noticed that the significance level of 97% for M2 cannot rule out the existence of the additional planets and/or bodies, because the feasibility of using the TTV technique to detect additional planets in the transiting system depends on the physical and orbital properties of the multiple planet system, the accuracy of transit timing and the time span of observations (Holman & Murray 2005).

We compute the age of WASP-32 using the isochrone interpolation routine based on the Yonsei-Yale (Y^2) models (Yi et al. 2001; Demarque et al. 2004). Since our stellar mean density is smaller, we derive an older stellar age of 2.65 ± 1.35 Gyr. This is consistent with the value of $2.22^{+0.62}_{-0.73}$ Gyr, which was derived by Brown et al. (2012) using the same stellar evolutionary model. Relying on the estimation of the age of WASP-32, we can compare our measurement with the theoretical model of Fortney et al. (2007). We translate the separation $a = 0.0395$ AU between the planet and the host star of WASP-32 into the distance $d_\odot = 0.0328$ AU, where the planet receives equivalent irradiation from the Sun (see equations 9 and 10 in Fortney et al. (2007)) before comparing our derived planet radius with the theoretical value. Comparing with the theoretical radius $R_{\rm th} = 1.20\,R_{\rm Jup}$ of a coreless planet at 1 Gyr (Fortney et al. 2007), we cannot derive a more convincing result about WASP-32b other than a non-inflated planet because of the rather sizable uncertainties in the radius of WASP-32b and the age of the system.

6 SUMMARY

From the above homogenous analysis for our new photometric observations and the published light curves and radial velocity curves, we have obtained new physical parameters of WASP-32, which are consistent with those of Maxted et al. (2010) and have slightly higher accuracy. Through combining HARPS high-precision radial velocity data of Brown et al. (2012) with those of Maxted et al. (2010), we demonstrate that the orbit of WASP-32b should be circular. Via the $(O - C)$ analysis of mid-transit times, a more accurate orbital period is derived, and no apparent TTV signal is revealed from the presented mid-transit times.

Acknowledgements We thank the staff of the 1 m telescope at Yunnan Observatories and the staff of the 0.5 m telescope at Ho Koon Nature Education cum Astronomical Centre for supporting our observations. We also thank P.F.L. Maxted and P.V. Sada for generously providing us with their data. This work is supported by the National Natural Science Foundation of China (Grant No. 10873031) and Chinese Academy of Sciences through Project KJCXZ-YW-T24.

References

Agol, E., Steffen, J., Sari, R., & Clarkson, W. 2005, MNRAS, 359, 567
Anderson, D. R., Collier Cameron, A., Hellier, C., et al. 2011, ApJ, 726, L19
Baraffe, I., Chabrier, G., & Barman, T. 2008, A&A, 482, 315
Baraffe, I., Chabrier, G., & Barman, T. 2010, Reports on Progress in Physics, 73, 016901
Brothwell, R. D., Watson, C. A., Hébrard, G., et al. 2014, MNRAS, 440, 3392
Brown, D. J. A., Collier Cameron, A., Díaz, R. F., et al. 2012, ApJ, 760, 139
Carter, J. A., & Winn, J. N. 2009, ApJ, 704, 51
Claret, A. 2000, A&A, 359, 289
Claret, A. 2004, A&A, 428, 1001
Collier Cameron, A., Pollacco, D., Street, R. A., et al. 2006, MNRAS, 373, 799
Collier Cameron, A., Wilson, D. M., West, R. G., et al. 2007, MNRAS, 380, 1230
Demarque, P., Woo, J.-H., Kim, Y.-C., & Yi, S. K. 2004, ApJS, 155, 667
Enoch, B., Collier Cameron, A., & Horne, K. 2012, A&A, 540, A99
Enoch, B., Collier Cameron, A., Parley, N. R., & Hebb, L. 2010, A&A, 516, A33
Ford, E. B. 2005, AJ, 129, 1706
Ford, E. B., & Gaudi, B. S. 2006, ApJ, 652, L137
Fortney, J. J., Marley, M. S., & Barnes, J. W. 2007, ApJ, 659, 1661
Gazak, J. Z., Johnson, J. A., Tonry, J., et al. 2011, Transit Analysis Package (TAP and autoKep): IDL Graphical User Interfaces for Extrasolar Planet Transit Photometry, Astrophysics Source Code Library
Holman, M. J., & Murray, N. W. 2005, Science, 307, 1288
Jiang, I.-G., Yeh, L.-C., Thakur, P., et al. 2013, AJ, 145, 68
Kipping, D. M. 2009, MNRAS, 392, 181
Lucy, L. B., & Sweeney, M. A. 1971, AJ, 76, 544
Maciejewski, G., Dimitrov, D., Neuhäuser, R., et al. 2010, MNRAS, 407, 2625
Maciejewski, G., Dimitrov, D., Seeliger, M., et al. 2013, A&A, 551, A108
Mandel, K., & Agol, E. 2002, ApJ, 580, L171
Maxted, P. F. L., Anderson, D. R., Collier Cameron, A., et al. 2010, PASP, 122, 1465
Miralda-Escudé, J. 2002, ApJ, 564, 1019
Mortier, A., Santos, N. C., Sousa, S. G., et al. 2013, A&A, 558, A106
Pollacco, D., Skillen, I., Collier Cameron, A., et al. 2008, MNRAS, 385, 1576
Sada, P. V., Deming, D., Jennings, D. E., et al. 2012, PASP, 124, 212
Seager, S., & Mallén-Ornelas, G. 2003, ApJ, 585, 1038
Sozzetti, A., Torres, G., Charbonneau, D., et al. 2007, ApJ, 664, 1190
Tamuz, O., Mazeh, T., & Zucker, S. 2005, MNRAS, 356, 1466
Tan, H.-B., Wang, X.-B., Gu, S.-H., & Cameron., A. C. 2013, Acta Astronomical Sinca, 54, 527
Torres, G., Andersen, J., & Giménez, A. 2010, A&A Rev., 18, 67
Torres, G., Fischer, D. A., Sozzetti, A., et al. 2012, ApJ, 757, 161
Torres, G., Winn, J. N., & Holman, M. J. 2008, ApJ, 677, 1324
Wang, X.-B., Gu, S.-H., Collier Cameron, A., et al. 2013, RAA (Research in Astronomy and Astrophysics), 13, 593
Wang, X.-b., Gu, S.-h., Collier Cameron, A., et al. 2014, AJ, 147, 92
Winn, J. N., Holman, M. J., Torres, G., et al. 2008, ApJ, 683, 1076
Yi, S., Demarque, P., Kim, Y.-C., et al. 2001, ApJS, 136, 417